Computers in Biology and Medicine 187 (2025) 109722

Contents lists available at ScienceDirect

Computers in Biology and Medicine

journal homepage: www.elsevier.com/locate/compbiomed

Dynamic blinking feature extraction for automated facial nerve paralysis detection

Akara Supratak [a], Watsaporn Pornwatanacharoen [b], Varit Rungbanapan [a], Skonlawut Tasnaworanun [a], Rachata Chopdamrongtham [a], Thanapon Noraset [a], Manachaya Prukajorn [b], Pimkwan Jaru-ampornpan [b,*]

[a] Faculty of Information and Communication Technology, Mahidol University, 999 Phuttamonthon 4 Road, Nakhon Pathom, 73170, Thailand
[b] Department of Ophthalmology, Faculty of Medicine Siriraj Hospital, Mahidol University, 2 Wang Lang Road, Bangkok, 10700, Thailand

ARTICLE INFO

Keywords:
Facial nerve paralysis
Machine learning
High-frame-rate video
Blinking
Dynamic blink parameters

ABSTRACT

Facial nerve paralysis (FNP) impair eyelid closure and blinking, risking ophthalmic complications and vision loss. Current detection methods primarily rely on static facial asymmetries, overlooking the dynamic eyelid movements during blinking that are important for evaluating treatment outcomes such as blink restoration. In this study, we present an automated system for objectively extracting dynamic blink features from high-frame-rate videos to address these limitations. We develop algorithms for dynamic blink feature extraction using a facial landmark detection model to capture eyelid movements and derive parameters for each blink. These parameters are processed with an Isolation Forest model to learn the typical distribution of combined parameters from both eyes, generating normality scores for each blink pair to indicate the degree of abnormality in upper eyelid movement while reducing noise from landmark detection and head movements. Our evaluation, which included 103 subjects (86 healthy and 17 with FNP), shows that the machine learning model trained to detect FNP using normality scores outperformed those trained with static parameters (with an increase of 75% in F1-score) and dynamic parameters (with an increase of 35% in F1-score). Notably, the normality score of the closing blink velocity, representing the speed at which the upper eyelid margin moves during the eye-closing phase, was the most distinguishing feature for FNP detection. These findings highlight the potential of the dynamic blink features in FNP detection and suggest further exploration to assess their effectiveness as objective measures for diagnosing FNP in addition to the facial asymmetry features proposed in other studies.

1. Introduction

Facial nerve paralysis (FNP) is characterized by dysfunction in the facial muscles, including the orbicularis oculi muscle [1]. This muscle, innervated by the facial nerve, plays a vital role in normal eyelid closure and blinking. Abnormal blink characteristics in FNP encompass reduced movements in both the upper and lower eyelids on the affected side [2], along with a reduction in the magnitude of the orbicularis oculi muscle contraction and a slowing of the peak velocity during the closing phase [3]. The presence of abnormal and incomplete blinking in FNP can lead to various ophthalmic complications, including exposure to keratitis, corneal ulceration, and potential loss of vision if not managed appropriately. Ocular management for FNP involves ocular surface lubrication and surgical interventions aimed at improving static eyelid position or restoring dynamic blink, such as eyelid weight placement. However, diagnosing abnormal blinks or assessing treatment efficacy, especially in individuals with milder FNP, can sometimes be challenging.

Traditionally, the electromagnetic search coil technique has been prominently used to record orbicularis oculi electromyography (OO-EMG). This method describes upper eyelid movement and is employed for measuring objective blink parameters such as blink amplitude, duration, maximum velocity, and latency from OO-EMG activity to blink onset [4]. However, its popularity declined due to the inconvenience of wire coil attachment and the disruption of natural blinking [5]. Moreover, OO-EMG requires specialized equipment and expertise, which limits its clinical accessibility. There remains a critical need for an accurate, automated, minimally invasive, and objective evaluation method for FNP diagnosis that can distinguish FNP patients from healthy subjects and quantify the severity of their condition.

* Corresponding author.
E-mail address: pimkwan.jar@mahidol.edu (P. Jaru-ampornpan).

https://doi.org/10.1016/j.compbiomed.2025.109722
Received 15 July 2024; Received in revised form 16 January 2025; Accepted 17 January 2025
Available online 5 February 2025

Recently, many studies have developed automated systems based on machine learning to aid in diagnosing FNP using facial images, which can be grouped into two types: FNP detection and FNP severity classification. FNP detection is a binary classification task aimed at determining whether a subject has an FNP condition. Most existing works have hand-engineered facial symmetry/asymmetry features from facial landmarks extracted from a set of still images of different expressions [6–9]. Additionally, a recent study has developed an end-to-end deep learning model for FNP detection using raw facial images from videos, bypassing the need for hand-engineered features [10]. FNP severity classification, on the other hand, is a multi-class classification task that assesses the severity of FNP in a subject. They have employed the 2D/3D facial landmark detection models to extract and aggregate features from a set of pre-defined facial expressions to represent the severity of each patient [9,11]. Several studies have utilized the deep learning model to automatically learn useful features from raw still images of several facial expressions for paralysis grading without the facial landmark detection models [12,13]. Existing research on both FNP detection and classification primarily focuses on facial asymmetry characteristics derived from still images, commonly referred to as static features. However, these static features do not capture the dynamic movement of blinking characteristics as the electromagnetic search coil method. Dynamic parameters, such as blinking velocity, derived from the movements of eyelids during blinks in video recordings, are important indicators of outcomes, including the success of blink restoration procedures [14–16]. Yet, these dynamic features have been largely overlooked. To date, no study has developed an automated system capable of detecting subtle changes in eyelid movement during blinking. We believe that automating the extraction of dynamic blink parameters is crucial for the early detection of FNP. Additionally, it would assist in better tracking and improvement over follow-up or treatment by accurately capturing subtle changes in blinking characteristics.

High-frame-rate video cameras have become popular for analyzing blinking movements [17–20] and blinking related conditions such as facial paralysis [2], Parkinson's disease [21], and hermifacial spasm [22] due to their versatility, ease of use, and minimal interference. Studies have shown that they are just as reliable as the electromagnetic search coil technique [5]. The Terzis and Bruno Scoring System is an assessment that utilizes a blink video recording to assess blink ability following surgical intervention through the blink amplitude, a ratio of the distance during a complete blink attempt divided by interpalpebral distance at rest, and the coordination between both eyes [23]. However, the blinking periods were determined via a visual inspection, and the amplitude and ratio were measured manually from a freeze-framed image using a metric ruler on the monitor, which is labor-intensive and time-consuming. The electronic clinician-graded facial function scale (eFACE) is considered a relatively reliable tool for assessing facial nerve function and symmetry to compare the outcomes of surgical procedures based on a visual inspection of video recordings of subjects performing facial expressions [24,25]. Despite its capability of offering blink parameters, such as heights at rest, the scores of narrowing of palpebral fissure width at gentle/full eye closure for assessing eyelid function post-blink restoration procedures, it still rely on manual, subjective image grading by clinicians [26]. Additionally, they focused on static blink parameters, overlooking dynamic parameters derived from eyelid movements, such as blink rate, duration, phase, velocity, and incomplete blink count [27,28]. Recent studies have begun leveraging eyelid movements to detect blink completeness. For example, segmentation models have been trained to extract sequences of palpebral fissure heights and iris diameters in pixels for determining complete or incomplete blink counts [29]. Similarly, recurrent neural networks (RNNs) have been trained to analyze sequences of blinking frames from videos and classify each blink as complete or incomplete [30,31]. However, other dynamic blink parameters derived from eyelid movements have yet to be fully explored.

In this study, we introduce an automated system designed to objectively extract dynamic blink features from high-frame-rate blinking videos for FNP detection. We develop a dynamic blink feature extraction algorithm to derive parameters such as blink amplitude, blink phase duration, blink velocity, and closed-eye coverage area. These parameters rely on signals of upper eyelid movement, derived from sequences of facial landmarks extracted from video frames. To enhance the robustness of our features, we transform these parameters from both eyes of each blink into normality scores using an unsupervised learning algorithm. This approach helps mitigate noise from the facial landmark detection model and the movement of the patient's face during video recording. These normality scores are then averaged per patient and employed to train a machine learning model to distinguish between healthy subjects and those with FNP. Our evaluation, involving 103 subjects (86 healthy and 17 with FNP), demonstrated that the machine learning model trained with the normality scores outperformed those trained with static and dynamic blink parameters. This approach has the potential to improve diagnostic tools for FNP, allowing us to monitor changes in facial nerve function over time and evaluate the outcomes of blink restoration procedures. The code to reproduce this work is publicly available at Github.[1]

2. Material and method

2.1. Dataset

The dataset for this study was obtained following ethical approval (COA No. SI456/2019) and adherence to the principles of the Declaration of Helsinki. Participants, aged between 18 and 79 years (mean age 48.7, standard deviation 15.3), were recruited between July 2019 and November 2023. The dataset comprises 103 participants, categorized as either normal or facial nerve paralysis cases, with 86 (42 male, 44 female) individuals classified as normal and 17 (7 male, 10 female) as having facial nerve paralysis. Participants were excluded from the normal group if they had ocular surface disorders, eyelid conditions, or blink-related eye diseases (e.g., dry eye, thyroid eye disease, blepharospasm, Parkinson's), uncorrected visual acuity worse than 20/200, Marginal Reflex Distance (MRD1) less than 1 mm, ongoing use of topical ocular medications (except occasional artificial tears), or unresolved clinical diagnoses. Additionally, individuals with a history of eyelid surgery, trauma, or periocular botulinum toxin injections were excluded from both the normal and facial nerve paralysis groups.

Each participant completed a dry eye disease screening questionnaire before undergoing recording sessions using specialized equipment, including a modified camera setup (GoPro Hero 6 Black Camera with an 8.25 mm f/3.0 41d HFOV non-distortion lens) and controlled lighting conditions. A green paper measuring 2×2 cm was placed at the center of the subject's forehead before data collection. This green paper was used as a reference to determine the number of pixels equivalent to two centimeters in the video, enabling us to convert pixel-based dynamic blink parameters into millimeters. Facial photographs were taken, followed by video recordings capturing spontaneous blinks.

The participants were instructed to gaze straight ahead through the ring light, focusing on the monitor positioned 6 ft away, which displayed a video clip featuring a natural scene to induce relaxation. The video recording mode was set to capture 240 frames per second. Following a 30-s period of viewing the natural scene, spontaneous blink recordings were collected over a 90-s duration using a smartphone-controlled GoPro camera. Throughout this process, subjects remained unaware of the commencement of the video recording. At the end, the middle 30 s of the video recording were extracted and used in this study.

[1] The code will be available upon the publication of this manuscript.

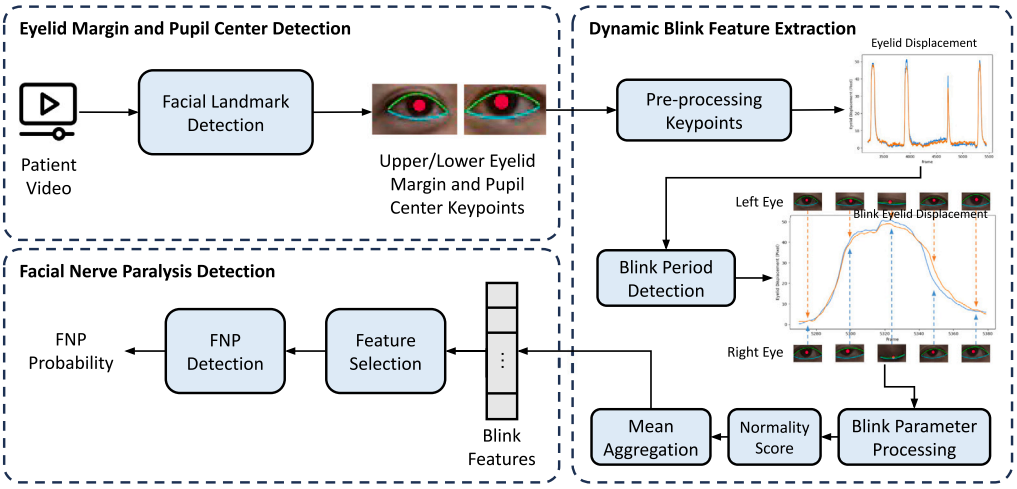

Fig. 1. Overview of the proposed method. Three main components are involved in transforming a high-frame-rate participant blinking video into the probability of having facial nerve paralysis (FNP). The first component, "Eyelid Margin and Pupil Center Detection", converts the high-frame-rate participant blinking video into a sequence of keypoints that represent the movement of the upper and lower eyelid margins, as well as the pupil center, throughout all frames in the video. The second component, "Dynamic Blink Feature Extraction", derives a range of blink-related features from the sequence of keypoints. These features are then aggregated for each participant, resulting in a set of blink features unique to each individual. The final component, "Facial Nerve Paralysis Detection", employs the extracted features from all participants to construct a binary classification model. This model predicts the probability of FNP, distinguishing between those who may have the condition and those who do not.

2.2. System overview

The proposed method consists of three main components: (1) *Eyelid Margin and Pupil Center Detection*, (2) *Dynamic Blink Feature Extraction*, and (3) *Facial Nerve Paralysis Detection* (see Fig. 1). Given an input high-frame-rate participant blinking video, the first component converts the high-frame-rate participant blinking video into a sequence of keypoints that represent the movement of the upper and lower eyelid margins, as well as the pupil center, throughout all frames in the video. The second component extracts a range of blink-related features from the sequence of keypoints for each participant. Based on the extracted blink features, the final component predicts whether the participant has FNP.

2.3. Eyelid Margin and Pupil Center Detection

This component extracts the sequence of keypoints representing the movement of eyelid margins of the left and right eyes from a high-frame-rate video. We employed a facial landmark detection tool, named MediaPipe,[2] to extract facial keypoints (i.e., the pairs of (x, y)) from the sequence of frames. For each frame, we obtain keypoints for the left and right eyes. This includes sixteen keypoints from the eyelid margins and four keypoints around the pupil (see Fig. 2). The eyelid margin keypoints are divided into upper and lower sections. During our experiment, we found noise in facial keypoints detected by MediaPipe, which was significantly influenced by lighting conditions, skin tone, and wrinkles around the eyelid area. This issue is likely due to MediaPipe being trained under conditions different from those in our study's data collection setup. As noisy keypoints can result in inaccurate estimates of dynamic blink parameters in subsequent processes, we addressed this by smoothing the eyelid lines using a degree-2 least square polynomial fit, resulting in a more precise representation of the eyelid margins. The pupil center is determined by finding the midpoint along the x and y axes of the four pupil keypoints. This process results in a sequence of keypoints representing the movement (i.e., changes in keypoints over time) of the upper eyelid margin, lower eyelid margin, and pupil center from all frames in the video (see Fig. 2).

[2] https://developers.google.com/mediapipe.

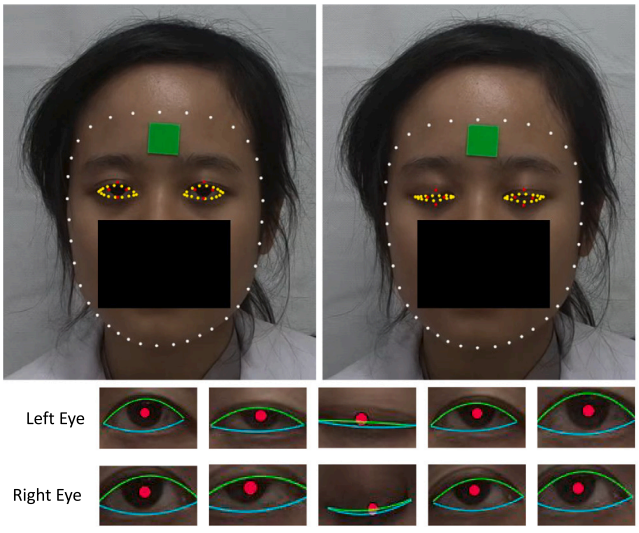

Fig. 2. Top: Examples of keypoints detected by MediaPipe, including facial landmarks (white dots), eyelid margins (yellow dots), and pupils (red dots) during the eye-opening (top-left) and eye-closing (top-right) phases. These keypoints are used to guide the cropping of the eye regions. **Bottom**: Example showing the curve-fitted upper (green line) and lower (cyan line) eyelid margins, along with the pupil centers (red dots) for both the left and right eyes.

2.4. Dynamic Blink Feature Extraction

Given a sequence of keypoints of the eye movements, Dynamic Blink Feature Extraction processes the sequence in five steps as detailed in the following.

2.4.1. Pre-processing keypoints

Before we extract blink features from the sequence of keypoints of the eyelid margins, we mitigate the errors from the facial landmark detection model and reduce the noises from the slight movement of the human face during the recordings.

We extract *eyelid displacement signals* from the sequence of eyelid margin keypoints. Initially, we extract the center keypoints of the upper eyelid margin, using the pupil center as a reference. These

keypoints serve as reference points for the eyelid movement. To address the jitter in keypoints, likely caused by sudden changes in lighting (potentially due to the high-frame-rate setting of the GoPro camera) and variations in head position over a sequence of frames, we apply a 4th order Butterworth band-pass filter [32] in the frequency range of 0.5 Hz to 6 Hz. This filtering process eliminates low-frequency non-stationary drifts and reduces high-frequency artifacts unrelated to blink movements. Fig. 3 illustrates examples of eyelid displacement signals from the left and right eyes of normal and FNP participants. These displacement signals and the sequence of keypoints are used to obtain more robust blink features in the subsequent steps.

2.4.2. Blink period detection

After preprocessing the eyelid displacement signals, the next step involves segmenting these signals to identify individual blink periods with significant eyelid movement. We begin by identifying continuous periods in the displacement signals where values exceed 0. Each period must last at least 0.04 milliseconds (ms), or 10 frames at 240 fps, with a minimum interval of 0.06 ms (15 frames at 240 fps) between consecutive periods. This ensures that blinks are neither too brief (under 0.04 ms) nor too close together (intervals under 0.06 ms). Then, we examine whether these periods contain only one peak (i.e., the point of eye closure) per period. These steps ensure that each identified period corresponds to a noticeable blink movement and filters out any false positives (e.g., short and noisy fluctuation periods). The extracted set of blink signals from each eye is denoted as $\mathbf{b}_1^l, \dots, \mathbf{b}_n^l$ for the left eye and $\mathbf{b}_1^r, \dots, \mathbf{b}_n^r$ for the right eye, where n is the number of blinks identified, $\mathbf{b}_i \in \mathbb{R}^m$ is a sequence of eyelid displacement values, and m is the number of frames per blink period. It should be noted that n and m vary across participants and blinks, respectively. Fig. 3 illustrates blink signals extracted from normal and facial nerve paralysis participants.

2.4.3. Blink parameter processing

To capture the abnormal blink characteristics in facial nerve paralysis participants, we extract the following blink parameters for each $\mathbf{b}_i$:

1. **Blink amplitude.** The blink amplitude represents how much participants can close their upper eyelid. The blink amplitude of the $\mathbf{b}_i$ can be estimated by:

$$max(\mathbf{b}_i) - min(\mathbf{b}_i) \tag{1}$$

2. **Blink phase duration.** The signal in each blink period was first divided into three phases: closing, start opening, and end opening.
   (a) **Closing phase.** This phase begins at the start of the blinking period and continues until reaching the peak of the displacement representing when the eye is closed.
   (b) **Start opening phase.** This phase begins at the peak of the displacement and extends until the eyelid displacement reaches half of the blink amplitude.
   (c) **End opening phase.** This phase comprises the remaining values until the end of the blink period.

   To determine the duration of each phase, we divide the number of values in each phase by the video's frame rate per second (fps). In this study, the fps is 240.
3. **Blink velocity.** The signal is divided into two parts based on the peak eyelid displacement in each blink period. This division separates the closing and opening phases of the blink. To determine the blink velocity for each phase, we calculate the maximum absolute difference in displacement values between two consecutive points within each phase. This process results in a **closing blink velocity** and an **opening blink velocity** representing the speed of the upper eyelid during each blink's closing and opening phases, respectively.
4. **Closed-eye coverage area.** The closed eye coverage area is a feature that quantifies the extent to which a participant can fully close their eye during a blink. We hypothesize that participants with abnormal blinks may experience difficulty in completely closing their eyes. To calculate the closed eye coverage area, we divide the distance between the center keypoints of the upper and lower eyelid margins at the peak index (the closed eye index) by the maximum distance between them when the eye is fully opened during the blink.

This process transforms from $\{\mathbf{b}_1^l, \dots, \mathbf{b}_n^l\}$ and $\{\mathbf{b}_1^r, \dots, \mathbf{b}_n^r\}$ to $\{\mathbf{r}_1^l, \dots, \mathbf{r}_n^l\}$ and $\{\mathbf{r}_1^r, \dots, \mathbf{r}_n^r\}$ where $\mathbf{r}_i \in \mathbb{R}^q$ is the vector of the blink parameters extracted from $\mathbf{b}_i$, and q is the number of parameters of each eye (in this study, $q = 7$).

Once the blink parameters from left and right eyes are obtained for p participants, they are represented as $\mathbf{R} = \{\mathbf{R}^{(k)}\}_{k=1}^{p}$, where:

$$\mathbf{R}^{(k)} = \{(\mathbf{r}_i^l \parallel \mathbf{r}_i^r)\}_{i=1}^{n_k} \tag{2}$$

is a matrix of size $n_k \times 2q$ (i.e., $\mathbf{R}^{(k)} \in \mathbb{R}^{n_k \times 2q}$), containing the blink parameters for the kth participant. Here n_k denotes the number of blinks recorded for the kth participant, and each row in $\mathbf{R}^{(k)}$ corresponds to the column-wise concatenation ($\parallel$) of the blink parameter vectors for the left ($\mathbf{r}_i^l$) and right ($\mathbf{r}_i^r$) eyes during the ith blink. To simplify notation, let N_b represent the total number of blink across all p participants, where $N_b = \sum_{k=1}^{p} n_k$. Thus, the combined blink parameter matrix $\mathbf{R}$ is of size $N_b \times 2q$ (i.e., $\mathbf{R} \in \mathbb{R}^{N_b \times 2q}$), where each row corresponds to the concatenated blink parameter vectors from a single blink across all participants.

2.4.4. Normality scores

Due to the noises from the facial landmark detection model and the movement of the participant's face during the video recordings, the direct use of the blink parameters from the previous step shows a sub-optimal performance. We propose mitigating such noise by converting pairs of blinking parameters from both eyes during the same blinking periods into *normality scores*, representing the degree of abnormality in combined upper eyelid movements. Our experiments show that utilizing normality scores instead of raw blink parameters significantly improves FNP detection performance.

We employ the Isolation Forest algorithm [33], an unsupervised anomaly detection algorithm, to learn the typical distribution of combined blink parameters from both eyes (see Algorithm 1) and generate the normality scores for each blink parameters (see Algorithm 2). For instance, to calculate normality scores for blink amplitudes, we first train the Isolation Forest model using blink amplitudes from all blinks across participants in the training set, allowing it to learn the typical distribution of combined blink amplitudes from both eyes (Line 3–7 in Algorithm 1). The trained model is then used to transform each pair of blink amplitudes from the left and right eyes into normality scores (Line 3–6 in Algorithm 2). This process is applied to each blink parameter.

In addition to calculating normality scores for each parameter, we also compute a composite normality score by training the Isolation Forest model on the full set of blink parameters from both eyes (Line 9–10 in Algorithm 1) to evaluate the overall normality across all blink parameters (Line 8 in Algorithm 2). This composite normality score, referred to as the **blink feature normality score**, provides a comprehensive assessment of the eyelid movement.

This process transforms the blink parameters from both left and right eyes of the kth participant, $\mathbf{R}^{(k)} \in \mathbb{R}^{n_k \times 2q}$, into normality scores, $\mathbf{A}^{(k)} \in \mathbb{R}^{n_k \times (q+1)}$. It is important to note that only the blink signals from participants in the training set are used to train the IsolationForest model. The trained IsolationForest model is then applied to compute normality scores for participants in the training set, test set, and any unseen participants.

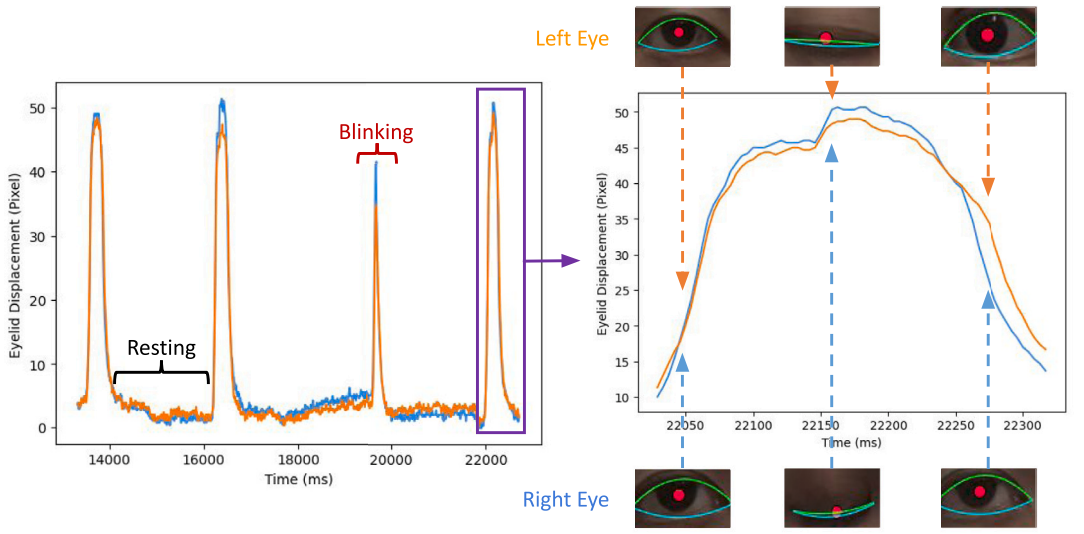

(a) Normal participant.

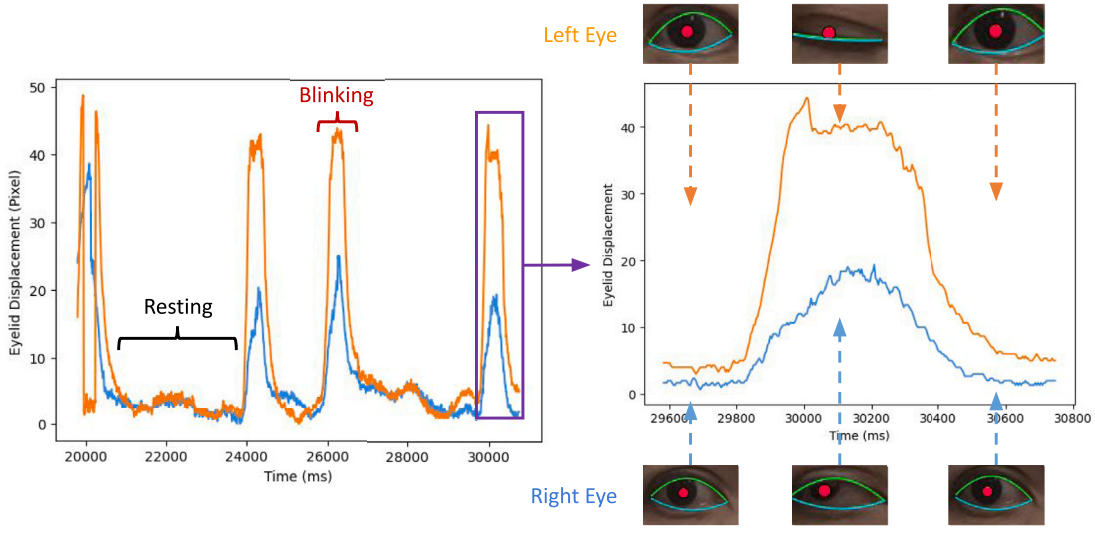

(b) FNP participant.

Fig. 3. Examples of the eyelid displacement signals during four blink periods from the pre-processing keypoint part (left), and the displacement signals of blink periods (right), i.e., $\mathbf{b}_i$, from the blink period detection part for a normal (a) and FNP (b) participant. Peaks in the signals represent eye closure points, while non-peak values near 0 indicate resting periods. The discrepancy between the displacement graphs of the left and right eyes is evident, particularly in the FNP participant, indicating the impaired ability of the right eye. These signals provide reliable features for detecting FNP.

Algorithm 1: Training IsolationForest Models

Data: Combined blink parameters $\mathbf{R}$.
Result: A set of trained IsolationForest F.

$F \leftarrow \emptyset$
for $j \leftarrow 1$ **to** q **do**
  // For each blink parameter
  $leye \leftarrow$ extract_column($\mathbf{R}, j$) // left eye
  $reye \leftarrow$ extract_column($\mathbf{R}, 2j$) // right eye
  $eye\_params \leftarrow leye \cup reye$ // combine parameters
  $f_j \leftarrow$ IsolationForest.train(eye_params)
  $F \leftarrow F \cup f_j$
end
$f_{q+1} \leftarrow$ IsolationForest.train($\mathbf{R}$)
$F \leftarrow F \cup f_{q+1}$

Algorithm 2: Computing Normality Scores

Data: Blink parameters for the k-th participant $\mathbf{R}^{(k)}$, and a set of trained IsolationForest F.
Result: Normality scores for the k-th participant $\mathbf{A}^{(k)}$.

$\mathbf{A}^{(k)} \leftarrow O$ // a zero matrix of size $n_k \times (q+1)$
for $j \leftarrow 1$ **to** q **do**
  // Normality score for each parameter
  $leye \leftarrow$ extract_column($\mathbf{R}^{(k)}, j$) // left eye
  $reye \leftarrow$ extract_column($\mathbf{R}^{(k)}, 2j$) // right eye
  $eye\_params \leftarrow leye \cup reye$ // combine parameters
  $\mathbf{A}^{(k)}_{*,j} \leftarrow f_j$.score($eye\_params$) // assign to column j
end
// Blink feature normality score
$\mathbf{A}^{(k)}_{*,q+1} \leftarrow f_{q+1}$.score($\mathbf{R}^{(k)}$) // assign to column $q+1$

2.4.5. Mean aggregation

Once the normality scores are computed for n_k blinks in the kth participant (i.e., $\mathbf{A}^{(k)}$), the average normality score across all blinks is calculated to summarize the participant's overall blinking behavior. Let $\mathbf{x}^{(k)} \in \mathbb{R}^{q+1}$ represents a blink feature vector for the kth participant. The jth blink feature, $x_j^{(k)}$, is computed as the average of the jth normality score across all blinks as follows:

$$x_j^{(k)} = \frac{1}{n_k} \sum_{i=1}^{n_k} A_{i,j}^{(k)}, \tag{3}$$

where $A_{i,j}^{(k)}$ is the jth normality score from the ith blink of the kth participant. The resulting blink features, $\mathbf{x}^{(k)}$, will be used as inputs in the facial nerve paralysis detection task.

2.5. Facial Nerve Paralysis Detection

Our blink feature extraction algorithm extracts many characteristics of blinks from a video; this might result in overfitting when learning to detect facial nerve paralysis participants of the downstream machine-learning models. We perform a feature selection to filter out features unrelated to facial nerve paralysis prior the model training and prediction.

Feature Selection. We applied the statistical-based and the model-based feature selection algorithms to reduce the number of features [33] based on the training set of each cross-validation fold. The former was the univariate feature selection using the analysis of variance (ANOVA) F-value. The latter was based on the feature importance scores from RandomForest. The feature important scores from all folds were averaged to determine the ranking of each approach. The features with the lower ranks on both approaches were selected for FNP detection.

Model Training and Prediction. This study considers facial nerve paralysis detection as a supervised binary classification to distinguish between normal ($y = 0$) and facial nerve paralysis ($y = 1$) participants. Formally, suppose there are blink features from p participants $\{\mathbf{x}^{(1)}, \ldots, \mathbf{x}^{(p)}\}$, where $\mathbf{x}^{(i)} \in \mathbb{R}^{q+1}$ is the blink features for the ith participant. Our objective is to train a machine learning model that can estimate the probability of an individual having the facial nerve paralysis condition $\{\hat{y}^{(1)}, \ldots, \hat{y}^{(p)}\}$ where $\hat{y}^{(i)} \in [0, 1]$. A participant will be classified as having facial nerve paralysis if their predicted probability $\hat{y}^{(i)}$ exceeds the threshold of 0.5. Otherwise, they will be considered as normal. We utilized seven learning algorithms implemented in existing Python libraries [33–35], consisting of Logistic Regression (LogR), Support Vector Machine (SVM), RandomForest (RF), Gaussian Naive Bayes (GNB), LightGBM (LGB), and XGBoost (XGB).

In this study, the default parameters provided by the respective packages (Scikit-learn version 1.3, LightGBM version 3.3.3, and XGBoost version 1.7.0) were used for feature selection, model training, and prediction. The hyperparameters we varied included the choice of features and supervised machine learning algorithms, as discussed in Section 3.2.

3. Results

3.1. Experimental setup

Due to the small number of participants, we evaluated our model with a stratified 10-fold cross-validation to see how the model performed on all participants. The 103 participants were split into 10 folds, ensuring that each fold had an equal proportion of normal and FNP participants. Each fold contained approximately 10 participants, with 8–9 normal and 1–2 FNP participants. During each iteration of the cross-validation process, one fold was set aside as the test set, while the remaining nine folds were utilized for feature selection and model training. This process was repeated 10 times, with each fold as the test set once. The performance metrics were calculated by aggregating the results obtained from the test sets of all folds. It is important to note that each fold was split by participant, ensuring that no blinks from the same participant appeared in both the training and test sets. This setup also allows us to assess the generalizability of the trained model to new, unseen participants.

The performance metrics used to evaluate the NPH detection performance are:

- Confusion Matrix Components: True Positives (TP) represent correctly predicted FNP cases, while False Positives (FP) indicate normal cases incorrectly classified as FNP. True Negatives (TN) are non-FNP cases correctly identified, and False Negatives (FN) are FNP cases that were incorrectly classified as non-FNP.
- Accuracy (ACC): Evaluate the overall correctness of the model by calculating the proportion of correctly classified instances (both true positives and true negatives) out of the total number of instances.
- Precision (PR): Evaluate how well the model correctly predicts FNP conditions (false positive is important).
- Sensitivity (Sen) (also called Recall): Evaluate how well the model can capture all participants with FNP conditions (false negative is important).
- Specificity (Spec): Evaluate how well the model correctly predict normal conditions (true negatives is important).
- F1-Score (F1): A harmonic mean of precision and sensitivity, balancing the trade-off between these two metrics. It is particularly useful when dealing with imbalanced datasets, as it considers both false positives and false negatives.
- Area Under the Receiver Operating Characteristic Curve (AU-ROC): Evaluate the model's ability to distinguish between positive and negative classes across different thresholds.

The cross-validation procedure and performance metrics were applied in two experiments. The first experiment aimed to identify the best combination of feature sets and supervised machine learning algorithms, as outlined in Section 2.5. Once the optimal feature set and classifier were determined, the second experiment compared their FNP detection performance against existing static and dynamic features to highlight the advantages of using the proposed normality scores.

3.2. Experiment 1: FNP detection performance

Our analysis showed that not all of the extracted features were useful for FNP detection. The results from the statistical-based and model-based feature selection with the training set from all folds showed that two out of eight normality scores, the duration of the closing phase and the end opening phase, consistently ranked as the least important features. The ranks of the other six features varied between the two selection methods: the duration of the start opening phase, the opening blink velocity, the closing blink velocity, the blink amplitude, the closed-eye coverage area, and the blink feature normality score. According to these results, we explored whether using all features (i.e., *all*) or only the six selected features (i.e., *selected*) would result in superior performance.

When considering the overall performance in terms of ACC, F1 and AU-ROC (see Table 1), the best-performing model was the LGB trained on the selected six blink features (ACC = 0.98, PR = 0.94, Sen = 0.94, Spec = 0.99, F1 = 0.94 and AU-ROC = 0.96). We performed a two-sided independent t-test to compare the F1 performance of LightGBM with other top-performing supervised models and found the differences to be statistically significant (p-value < 0.01). It only misclassified two out of 103 participants with one false positive and one false negative. Even though the LogR model trained on the same selected features achieved a perfect PR and Spec of 1.0 (i.e., no false positive), it missed four FNP participants, which was unsuitable for automatic FNP screening. We further analyzed which of the selected features of the best model influences the FNP decision the most. The SHapley Additive

Table 1
Comparison among different learning algorithms with and without feature selection in facial nerve paralysis detection.

Model	Features	N	ACC	PR	Sen	Spec	F1	AUC–ROC	TP	FP	FN	TN
LN	All	103	0.91	0.72	0.76	0.94	0.74	0.85	13	5	4	81
LN	Selected	103	0.94	0.87	0.76	0.98	0.81	0.87	13	2	4	84
LogR	All	103	0.95	0.93	0.76	0.99	0.84	0.88	13	1	4	85
LogR	Selected	103	0.86	**1.00**	0.76	**1.00**	0.87	0.88	13	**0**	4	**86**
GNB	All	103	0.95	0.8	0.94	0.95	0.86	0.95	16	4	1	82
GNB	Selected	103	0.97	0.89	0.94	0.98	0.92	0.96	16	2	1	84
SVM	All	103	0.95	0.93	0.76	0.99	0.84	0.88	13	1	4	85
SVM	Selected	103	0.96	0.93	0.82	0.99	0.87	0.91	14	1	3	85
RF	All	103	0.94	0.87	0.76	0.98	0.81	0.87	13	2	4	84
RF	Selected	103	0.95	0.93	0.76	0.99	0.84	0.88	13	1	4	85
LGB	All	103	0.97	0.94	0.88	0.99	0.91	0.94	15	1	2	85
LGB	Selected	103	**0.98**	0.94	**0.94**	0.99	**0.94**	**0.96**	**16**	1	**1**	85
XGB	All	103	0.94	0.87	0.76	0.98	0.81	0.87	13	2	4	84
XGB	Selected	103	0.95	0.93	0.76	0.99	0.84	0.88	13	1	4	85

exPlanations (SHAP) value [36] was employed to rank the features according to their influence on the model's predictions. These SHAP values were calculated based on the model's predictions on the test set of each cross-validation fold. The most important feature of the LGB model, consistently ranked by the SHAP values on all folds, was the normality score of the closing blink velocity. This finding highlights the significance of the speed at which the upper eyelid margin moves during the closing phase as the most distinguishing factor between normal individuals and those with FNP.

When we investigated the causes of the two misclassifications from the LGB model, we found that the normality score of the closing blink velocity and the close-eye coverage area were positioned close to the decision boundary between the two groups. Still, they fell into opposite sides, as shown in Fig. 4(a). Further examination revealed that these two participants differed from the rest of their groups regarding their closing blink velocity. The false negative misclassification occurred for one FNP participant, whose closing blink velocity was within the normal range. Conversely, one normal participant was misclassified as having FNP due to their closing blink velocity being faster than most normal participants. We believe the issues of such borderline cases can be mitigated in clinical practice by reporting the probability of FNP alongside the predicted status. This additional information can help clinicians pay closer attention during diagnosis, particularly when the probability lies near the borderline, thereby reducing the risk of false positives and false negatives.

3.3. Experiment 2: Comparison with existing feature extraction techniques

To demonstrate the effectiveness of the proposed normality scores for blink features, we compare the FNP detection performance using our features with the commonly-used static and dynamic features that can be extracted from videos:

- **Static Features.** These are features that can be extracted from a single video frame, including the ocular surface area, the palpebral fissure (PF), and the MRD1 at rest. Since our study focuses on extracting features during blinking from videos and not static images, we did not capture images of different facial expressions during data collection. Instead, we extracted the static features during rest periods, which can be identified using the remaining frames from the blink period detection step.
- **Dynamic Features.** These are features extracted from a sequence of keypoints of the eyelid margins during the blink periods. They include the number of blinks, complete blinks and incomplete blinks, interblink interval, MRD1, PF, blink amplitude, blink velocity, ocular surface area, blink rate per minute, blink duration, as well as the duration and velocity in each blink phase (i.e., closing, start opening, and end opening) [27,28,37,38]. We also applied our preprocessing step in Sections 2.4.1 and 2.4.2 to mitigate the noises before extracting the features. The parameters that were extracted for each blinking periods were aggregated using the mean to represent the average value per participant before being used to train the machine learning model.

The results from Table 2 showed that our feature extraction techniques, whether using selected features (ACC/F1 = 0.98/0.94) or not (ACC/F1 = 0.97/0.91), achieved significantly better FNP detection performance than both the static (ACC/F1 = 0.83/0.19) and dynamic features (ACC/F1 = 0.85/0.59). As expected, the static features extracted during rest periods performed poorly, as symptoms are typically observable during blinking. For the dynamic features, we observed inconsistencies in the features extracted during blinking periods throughout the recording session. This inconsistency was mainly due to noise in the detected keypoints from the facial landmark model and the subject's head movement during the recording, particularly during blinking periods. The inconsistent extraction of features for the same subject significantly affects the representative mean of each feature (see Fig. 4). This highlights the potential benefit of converting dynamic blink parameters into their normality scores using an unsupervised learning algorithm, as this can help mitigate noise and improve FNP detection performance.

It is important to note that this comparison is not intended to establish the superiority of the proposed method over static features previously designed for extraction from a set of different facial expressions in the previous studies (as discussed in Section 4). This is because our study did not collect a full set of facial expressions from participants; instead, we extracted static features from a single video frame during the resting period. As a result, these features failed to capture asymmetry characteristics between the left and right eyes that occur during blinking. Consequently, the performance levels for static features in this study did not match those reported in the existing literature. The purpose of this comparison is to demonstrate the potential of the proposed approach when applied to blinking videos, demonstrating the superior performance of dynamic parameters and normality scores over static parameters in this context. Further investigation, incorporating both facial expression datasets and spontaneous blinking videos, is necessary to thoroughly compare their effectiveness in FNP detection and severity classification. This would help determine whether static features, dynamic features, or a combination of both can improve the performance of tracking disease progression and evaluating treatment effectiveness.

4. Discussion

This study presents a fully-automated system that leverages a facial landmark detection model to extract blink features for FNP detection from high-frame-rate blinking videos. The investigation identifies the new normality score of the closing blink velocity, representing the speed at which the upper eyelid margin moves during the eye-closing phase, as the most distinguishing feature for FNP detection. These

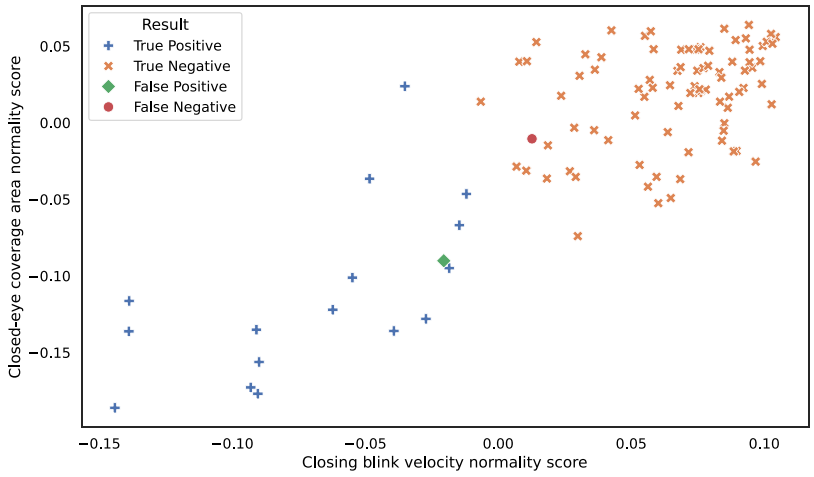

(a) Top two normality scores: closing blink velocity and closed-eye coverage area normality scores.

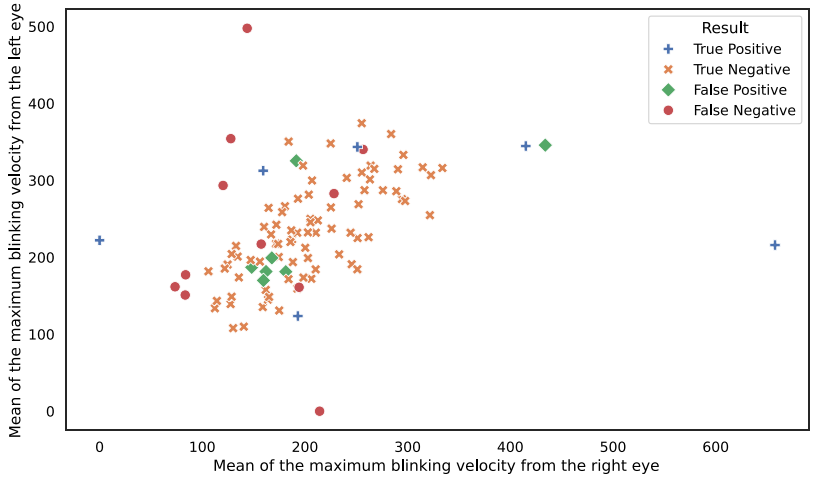

(b) Top two dynamic features: mean of the maximum blinking velocity from the left and right eyes.

Fig. 4. Comparison of the distribution of the top two features: (a) normality scores and (b) raw blink parameters. In (a), the true positives (blue plus) and true negatives (orange cross) are distinctly separated, indicating a clear decision boundary can be established between normal and FNP participants. In contrast, in (b), there is significant overlap, resulting in a higher occurrence of false positives (green diamond) and false negatives (red circle).

Table 2
Comparison of static, dynamic, and normality features in facial nerve paralysis detection.

Feature extraction	Model	N	ACC	PR	Sen	Spec	F1	AUC–ROC	TP	FP	FN	TN
Statics	LGB	103	0.83	0.5	0.12	0.98	0.19	0.55	2	15	2	84
Dynamics	GNB	103	0.85	0.55	0.65	0.9	0.59	0.77	11	9	6	77
Ours	LGB	103	0.97	0.94	0.88	0.99	0.91	0.94	15	1	2	85
Ours (selected)	**LGB**	**103**	**0.98**	**0.94**	**0.94**	**0.99**	**0.94**	**0.96**	**16**	**1**	**1**	**85**

findings highlight the significant potential of our dynamic blinking parameters, which have been previously overlooked in FNP studies, to improve the diagnosis of FNP. Moreover, our proposed system offers a novel platform for blink analysis, with the potential to seamlessly integrate into hospital FNP screening routines due to its automatic feature extraction capability that does not require manual annotation from the experts. This functionality makes it ideal for recording and analyzing patients' blinking videos while they wait in line, ensuring that when they consult with clinicians, the dynamic parameters are readily available to complement clinical assessments. The system's automatic and deterministic functionality can also reduce the variability inherent in subjective evaluations by clinicians, making it more suitable for extracting objective blinking parameters in FNP diagnosis. The system could be further enhanced to support the development of new diagnostic criteria and treatment strategies based on blinking characteristics, aiding ophthalmologists in managing not only FNP but also other blink-related conditions, such as dry eye, blepharospasm and Parkinson's disease, which may be subtle or challenging for clinicians to detect.

Our study makes a novel contribution to the field of automated FNP detection by introducing an approach that utilizes high-frame-rate videos to capture eyelid movements during spontaneous blinking (see Table 3). This stands in contrast to existing research, which relies either on manually engineered facial asymmetry features derived from predefined facial expressions [6–9] or automatically learned features from independent facial frames in videos using deep learning [10]. Visible asymmetries, such as differences in eyelid position with the eyes open and closed or overt facial droop, may not be present in mild or early cases of FNP. This is especially true for patients with minor trauma or localized nerve lesions, such as those affecting only the temporal branch of the facial nerve. Our method addresses this limitation by evaluating dynamic blinking parameters, such as blink

Table 3
Comparison of facial nerve paralysis detection methods.

Method	Feature type	Feature	Data type	Dataset	Subject
[6]	Static	Facial asymmetry features from facial landmarks	Video	Facial movement videos from their dataset	Normal vs. FNP
[7]	Static	Facial features extracted from SqueezeNet [39]	Image	Face images from YouTube Facial Palsy (YFP) [10] and Caltech Face dataset [40]	Normal vs. FNP
[8]	Static	Facial asymmetry features from facial landmarks	Image	Face images from Massachusetts Eye and Ear Infirmary (MEEI) [41] and Toronto NeuroFace (TNF) [25]	Normal vs. FNP
[10]	Static	Raw face images	Image	Face images from YouTube Facial Palsy (YFP) dataset [10]	FNP
[9]	Static	Facial asymmetry features from facial landmarks	Image	Face images from their dataset	Normal vs. FNP
Ours	Dynamic	Dynamic blinking features and normality scores from facial landmarks	Video	Blinking videos from our dataset	Normal vs. FNP

velocity, phase, and completeness, which can uncover subtle abnormalities that are often missed during visual assessments or static imaging. A key innovation of our approach is the use of normality scores, which provide valuable insights into abnormal movements during blinking. For example, features such as the normality score of the closing blink velocity were identified as key discriminators between normal and FNP participants, offering a significant advancement in the analysis of blinking-related conditions. These dynamic parameters enable a more comprehensive evaluation of eyelid function and can be further explored, in combination with static features, as objective measures for diagnosing FNP and assessing its severity.

Despite the promising results obtained from our experiments, our method has several limitations that need to be addressed. Firstly, the reliability of the extracted features heavily depends on the performance of the facial landmark detection model. Specifically, factors such as aging, wrinkles along the eyelids, and distorted eyelid margins caused by FNP or other conditions such as blepharospasm and Parkinson's disease can negatively impact keypoint prediction accuracy. This issue arises because the existing MediaPipe model has not been specifically trained to optimize keypoint accuracy along the eyelid margin, and its training set likely lacks participants with such conditions. Although we applied a band-pass filter to mitigate the jitter caused by the model, we still observed instances of sub-optimal keypoints detected during the blink periods. This may explain why using normality scores derived from the anomaly detection model instead of raw blink parameter values, consistently yields better results. Secondly, representing each participant with the mean of the blink features extracted from all blinks may be sub-optimal. Some blinks may not be fully representative of the participant's typical blinking behavior, yet they heavily influence the computed mean, potentially leading to less representative features.

These limitations highlight the necessity for refining our methodology. Although MediaPipe has the potential to generalize well across different ethnicities due to its training on diverse human facial structures, it may not perform as effectively for participants with wrinkles or distorted eyelid margins. Future work should prioritize fine-tuning the facial landmark detection model using clinician-annotated keypoints for abnormal/incorrect cases. Active learning techniques [42] could be employed to identify representative frames for annotation, reducing the burden of annotating large high-frame-rate blinking datasets. Another area for improvement involves how blink features are summarized at the participant level. Developing a more sophisticated approach to summarizing blink features could yield more accurate and representative features of each participant's blinking behavior. These improvements would enable the system to detect subtle changes in blink parameters, such as amplitude and velocity, which are important for detecting FNP, grading its severity, tracking disease progression, and evaluating treatment outcomes. Additionally, they would broaden its utility to include other blink-related conditions, such as blepharospasm and Parkinson's disease, significantly enhancing its clinical applicability.

5. Conclusion

This study is the first to explore the potential of dynamic blink features automatically extracted from high-frame-rate blinking videos for FNP detection. We develop a dynamic blink feature extraction algorithm to derive normality scores, quantifying abnormalities in the movement of the upper eyelid margins from sequences of facial landmarks extracted from video frames. The proposed normality score of the closing blink velocity, reflecting the speed of the upper eyelid margin during eye-closing, emerges as the most distinguishing feature for FNP detection. The LGB model, trained with six selected features, achieves excellent performance with only two misclassifications among 86 normal and 17 FNP participants. Moreover, the model trained with our normality scores outperformed those trained with static parameters (with an improvement of 15% in accuracy and 75% in F1-score) and dynamic parameters (with an improvement of 13% in accuracy and 35% in F1-score). These promising findings suggest the potential integration of this system into FNP screening routines in hospitals. Additionally, it opens up possibilities for extracting new features and developing novel diagnostic criteria and treatment strategies for ophthalmologists working with FNP patients.

In addition to the FNP condition, we believe the proposed blink features can also be extended to detect blink abnormality, track disease progression and evaluate treatment outcomes in patients with other blink-related conditions, such as dry eye, blepharospasm, and Parkinson's disease, which may be subtle or challenging for clinicians to detect. We plan to explore the possibility of utilizing these blink features to detect blink abnormality across various patients.

CRediT authorship contribution statement

Akara Supratak: Writing – review & editing, Writing – original draft, Visualization, Validation, Supervision, Software, Resources, Project administration, Methodology, Investigation, Funding acquisition, Formal analysis, Conceptualization. **Watsaporn Pornwatanacharoen:** Writing – original draft, Visualization, Data curation. **Varit Rungbanapan:** Writing – original draft, Visualization, Software, Methodology. **Skonlawut Tasnaworanun:** Writing – original draft, Visualization, Software, Methodology. **Rachata Chopdamrongtham:** Visualization, Software. **Thanapon Noraset:** Writing – review & editing, Validation, Supervision. **Manachaya Prukajorn:** Data curation. **Pimkwan Jaru-ampornpan:** Writing – review & editing, Writing – original draft, Validation, Supervision, Resources, Funding acquisition, Data curation, Conceptualization.

Ethics statement

This study was conducted following the ethical guidelines and principles outlined in the Declaration of Helsinki. Ethical approval for this study was obtained from the relevant institutional review board (COA No. SI456/2019). All participants provided written informed consent prior to participation after being thoroughly briefed about the study's objectives, procedures, and potential risks.

The dataset used in this study includes participants aged 18 to 79, recruited between July 2019 and November 2023. Exclusion criteria were established to ensure the reliability and relevance of the dataset, excluding individuals with ocular surface disorders, unresolved clinical diagnoses, or a history of eyelid surgery, trauma, or periocular botulinum toxin injections. Efforts were made to minimize discomfort and ensure the privacy and confidentiality of all participants.

All data collection procedures were conducted in controlled environments, including video recordings and dry eye disease screening questionnaires. The collected data were anonymized and securely stored to safeguard participant privacy. The use of a green reference patch during recordings served solely to facilitate pixel-to-millimeter conversions for analytical purposes.

The approved protocol and procedures ensured participant safety and ethical compliance throughout the study, and no adverse events were reported.

Declaration of competing interest

The authors declare that they have no known competing financial interests or personal relationships that could have appeared to influence the work reported in this paper.

Acknowledgments

This research project is supported by Siriraj research development fund, Grant Number (IO) R016238003, Faculty of Medicine Siriraj Hospital, Mahidol University, Thailand.

References

[1] A. Fattah, G.H. Borschel, R.T. Manktelow, M. Bezuhly, R.M. Zuker, Facial palsy and reconstruction, Plast. Reconstr. Surg. 129 (2) (2012) 340e, http://dx.doi.org/10.1097/PRS.0b013e31823aedd9.

[2] K. Ogawa, M. Okazaki, H. Mori, T. Hidaka, Y. Tomioka, K. Tanaka, N. Uemura, M. Akiyama, Comparative blink analysis in patients with established facial paralysis using high-speed video analysis., J. Craniofac. Surg. (2022) http://dx.doi.org/10.1097/scs.0000000000008326.

[3] P.A. Sibony, C. Evinger, C. Evinger, C. Evinger, K.A. Manning, Eyelid movements in facial paralysis, Arch. Ophthalmol. 109 (11) (1991) 1555–1561, http://dx.doi.org/10.1001/archopht.1991.01080110091043.

[4] C. Evinger, K.A. Manning, P.A. Sibony, Eyelid movements. mechanisms and normal data, Invest. Ophthalmol. Vis. Sci. 32 (2) (1991) 387–400.

[5] S.P. de Farias Wambier, S. Ribeiro, D.M. Garcia, R.R. Brigato, A. Messias, A.A. Velasco e Cruz, Two-dimensional video analysis of the upper eyelid motion during spontaneous blinking, Ophthal. Plast. Reconstr. Surg. 30 (2) (2014) 146–151, http://dx.doi.org/10.1097/iop.0000000000000031.

[6] H.S. Kim, S.Y. Kim, Y.H. Kim, K.S. Park, A smartphone-based automatic diagnosis system for facial nerve palsy, Sensors 15 (10) (2015) 26756–26768, http://dx.doi.org/10.3390/s151026756, Number: 10 Publisher: Multidisciplinary Digital Publishing Institute.

[7] O.O. Abayomi-Alli, R. Damaševičius, R. Maskeliūnas, S. Misra, Few-shot learning with a novel voronoi tessellation-based image augmentation method for facial palsy detection, Electron. 10 (8) (2021) 978, http://dx.doi.org/10.3390/electronics10080978, Number: 8 Publisher: Multidisciplinary Digital Publishing Institute.

[8] G.S. Parra-Dominguez, R.E. Sanchez-Yanez, C.H. Garcia-Capulin, Facial paralysis detection on images using key point analysis, Appl. Sci. 11 (5) (2021) 2435, http://dx.doi.org/10.3390/app11052435, Number: 5 Publisher: Multidisciplinary Digital Publishing Institute.

[9] J. Barbosa, W.-K. Seo, J. Kang, ParaFaceTest: an ensemble of regression tree-based facial features extraction for efficient facial paralysis classification, BMC Med. Imaging 19 (2019) 30, http://dx.doi.org/10.1186/s12880-019-0330-8.

[10] G.-S.J. Hsu, J.-H. Kang, W.-F. Huang, Deep hierarchical network with line segment learning for quantitative analysis of facial palsy, IEEE Access 7 (2019) 4833–4842, http://dx.doi.org/10.1109/ACCESS.2018.2884969, Conference Name: IEEE Access.

[11] A. Gaber, M.F. Taher, M.A. Wahe, N.M. Shalaby, S. Gaber, Classification of facial paralysis based on machine learning techniques, Biomed. Eng. Online 21 (1) (2022) http://dx.doi.org/10.1186/s12938-022-01036-0, 65–65.

[12] M. Sajid, T. Shafique, M.J.A. Baig, I. Riaz, S. Amin, S. Manzoor, Automatic grading of palsy using asymmetrical facial features: A study complemented by new solutions, Symmetry 10 (7) (2018) 242, http://dx.doi.org/10.3390/sym10070242, Number: 7 Publisher: Multidisciplinary Digital Publishing Institute.

[13] T.C. ten Harkel, G. de Jong, H.A.M. Marres, K.J.A.O. Ingels, C.M. Speksnijder, T.J.J. Maal, Automatic grading of patients with a unilateral facial paralysis based on the sunnybrook facial grading system - a deep learning study based on a convolutional neural network, Am. J. Otolaryngol. 44 (3) (2023) 103810, http://dx.doi.org/10.1016/j.amjoto.2023.103810.

[14] J.K. Terzis, D. Karypidis, Blink restoration in adult facial paralysis, Plast. Reconstr. Surg. 126 (1) (2010) 126, http://dx.doi.org/10.1097/PRS.0b013e3181dbbf34.

[15] M. Zaidman, C.B. Novak, G.H. Borschel, K. Joachim, R.M. Zuker, Assessment of eye closure and blink with facial palsy: A systematic literature review, J. Plast. Reconstr. Aesthetic Surg. 74 (7) (2021) 1436–1445, http://dx.doi.org/10.1016/j.bjps.2021.03.059.

[16] A. Gerós, R. Horta, P. Aguiar, Facegram – objective quantitative analysis in facial reconstructive surgery, J. Biomed. Inform. 61 (2016) 1–9, http://dx.doi.org/10.1016/j.jbi.2016.03.011.

[17] H. Pult, B.H. Riede-Pult, P.J. Murphy, P.J. Murphy, A new perspective on spontaneous blinks, Ophthalmol. 120 (5) (2013) 1086–1091, http://dx.doi.org/10.1016/j.ophtha.2012.11.010.

[18] J. Espinosa, B. Domenech, C. Vázquez, J. Pérez, D. Mas, Blinking characterization from high speed video records. application to biometric authentication, PLoS ONE 13 (5) (2018) http://dx.doi.org/10.1371/journal.pone.0196125.

[19] K. Radlak, B. Smolka, A novel approach to the eye movement analysis using a high speed camera, Int. Conf. Adv. Comput. Tools Eng. Appl. (2012) 145–150, http://dx.doi.org/10.1109/ictea.2012.6462854.

[20] W.-H. Lee, W.-K. Seo, J.-M. Hwang, The analysis of eye blinking pattern using high-frame-rate camera, in: Conference proceedings: 39th Annual International Conference of the IEEE Engineering in Medicine and Biology Society, Vol. 2017, 2017, pp. 1509–1512, http://dx.doi.org/10.1109/EMBC.2017.8037122.

[21] N. Kimura, A. Watanabe, K. Suzuki, H. Toyoda, N. Hakamata, H. Fukuoka, Y. Washimi, Y. Arahata, A. Takeda, M. Kondo, T. Mizuno, S. Kinoshita, Measurement of spontaneous blinks in patients with parkinson's disease using a new high-speed blink analysis system, J. Neurol. Sci. 380 (2017) 200–204, http://dx.doi.org/10.1016/j.jns.2017.07.035.

[22] M.H. Osaki, T.H. Osaki, D.M. Garcia, T. Osaki, G.R. Gameiro, R. Belfort, A.A.V. Cruz, Analysis of blink activity and anomalous eyelid movements in patients with hemifacial spasm, Graefe' s Arch. Clin. Exp. Ophthalmol. 258 (3) (2020) 669–674, http://dx.doi.org/10.1007/s00417-019-04567-w.

[23] J.K. Terzis, W. Bruno, Outcomes with eye reanimation microsurgery, Facial Plast. Surg. 18 (02) (2002) 101–112, http://dx.doi.org/10.1055/s-2002-32200, Publisher: Copyright © 2002 by Thieme Medical Publishers, Inc., 333 Seventh Avenue, New York, NY 10001, USA. Tel.: +1(212) 584-4662.

[24] C.A. Banks, P.K. Bhama, J. Park, C.R. Hadlock, T.A. Hadlock, Clinician-graded electronic facial paralysis assessment: The eFACE, Plast. Reconstr. Surg. 136 (2) (2015) 223e–230e, http://dx.doi.org/10.1097/PRS.0000000000001447.

[25] M.Q. Miller, T.A. Hadlock, E. Fortier, D.L. Guarin, The auto-eFACE: Machine learning–enhanced program yields automated facial palsy assessment tool, Plast. Reconstr. Surg. 147 (2) (2021) 467–474, http://dx.doi.org/10.1097/PRS.0000000000007572.

[26] K. Boochoon, A. Mottaghi, A. Aziz, J.-P. Pepper, Deep learning for the assessment of facial nerve palsy: Opportunities and challenges, Facial Plast. Surg. 39 (2023) 508–511, http://dx.doi.org/10.1055/s-0043-1769805, Publisher: Thieme Medical Publishers, Inc..

[27] K.J. Godfrey, C. Wilsen, K.R. Satterfield, B.S. Korn, D.O. Kikkawa, Analysis of spontaneous eyelid blink dynamics using a 240 frames per second smartphone camera., Ophthal. Plast. Reconstr. Surg. 35 (5) (2019) 503–505, http://dx.doi.org/10.1097/iop.0000000000001356.

[28] Y. Su, Q. Liang, G. Su, N. Wang, C. Baudouin, A. Labbé, Spontaneous eye blink patterns in dry eye: Clinical correlations, Invest. Ophthalmol. Vis. Sci. 59 (12) (2018) 5149–5156, http://dx.doi.org/10.1167/iovs.18-24690.

[29] G. Nousias, E.-K. Panagiotopoulou, K. Delibasis, A.-M. Chaliasou, A.-M. Tzounakou, G. Labiris, Video-based eye blink identification and classification, IEEE J. Biomed. Health Inf. 26 (7) (2022) 3284–3293, http://dx.doi.org/10.1109/JBHI.2022.3153407, Conference Name: IEEE Journal of Biomedical and Health Informatics.

[30] A. Fogelton, W. Benesova, Eye blink completeness detection, Comput. Vis. Image Underst. 176–177 (2018) 78–85, http://dx.doi.org/10.1016/j.cviu.2018.09.006.

[31] G. de la Cruz, M. Lira, O. Luaces, B. Remeseiro, Eye-LRCN: A long-term recurrent convolutional network for eye blink completeness detection, IEEE Trans. Neural Netw. Learn. Syst. 35 (4) (2024) 5130–5140, http://dx.doi.org/10.1109/TNNLS.2022.3202643, Conference Name: IEEE Transactions on Neural Networks and Learning Systems.

[32] S. Butterworth, On the theory of filter amplifiers, Wirel. Eng. 7 (6) 536–541.

[33] F. Pedregosa, G. Varoquaux, A. Gramfort, V. Michel, B. Thirion, O. Grisel, M. Blondel, P. Prettenhofer, R. Weiss, V. Dubourg, J. Vanderplas, A. Passos, D. Cournapeau, M. Brucher, M. Perrot, É. Duchesnay, Scikit-learn: Machine learning in python, J. Mach. Learn. Res. 12 (85) (2011) 2825–2830.

[34] G. Ke, Q. Meng, T. Finley, T. Wang, W. Chen, W. Ma, Q. Ye, T.-Y. Liu, Lightgbm: a highly efficient gradient boosting decision tree, in: Proceedings of the 31st International Conference on Neural Information Processing Systems, NIPS '17, Curran Associates Inc., Red Hook, NY, USA, 2017, pp. 3149–3157.

[35] T. Chen, C. Guestrin, Xgboost: A scalable tree boosting system, in: Proceedings of the 22nd ACM SIGKDD International Conference on Knowledge Discovery and Data Mining, KDD '16, Association for Computing Machinery, New York, NY, USA, 2016, pp. 785–794, http://dx.doi.org/10.1145/2939672.2939785.

[36] S.M. Lundberg, S.-I. Lee, A unified approach to interpreting model predictions, in: Advances in Neural Information Processing Systems, Vol. 30, Curran Associates, Inc., 2017.

[37] Y. Kim, H. Lew, Modified blink dynamic index predicts activity and severity in patient with facial nerve palsy, Front. Ophthalmol. 2 (2022) http://dx.doi.org/10.3389/fopht.2022.960593, Publisher: Frontiers.

[38] F.H.W. Mak, A.H. Harker, K.-A. Kwon, M. Edirisinghe, G.E. Rose, G.E. Rose, F. Murta, D.G. Ezra, Analysis of blink dynamics in patients with blepharoptosis, J. R. Soc. Interface 13 (116) (2016) 20150932, http://dx.doi.org/10.1098/rsif.2015.0932.

[39] F.N. Iandola, S. Han, M.W. Moskewicz, K. Ashraf, W.J. Dally, K. Keutzer, SqueezeNet: AlexNet-level accuracy with 50x fewer parameters and <0.5MB model size, 2016, http://dx.doi.org/10.48550/arXiv.1602.07360, arXiv:1602.07360 [cs].

[40] M. Weber, Caltech face dataset 1999, 2022.

[41] J.J. Greene, D.L. Guarin, J. Tavares, E. Fortier, M. Robinson, J. Dusseldorp, O. Quatela, N. Jowett, T. Hadlock, The spectrum of facial palsy: The MEEI facial palsy photo and video standard set, Laryngoscope 130 (1) (2020) 32–37, http://dx.doi.org/10.1002/lary.27986.

[42] H. Wang, Q. Jin, S. Li, S. Liu, M. Wang, Z. Song, A comprehensive survey on deep active learning in medical image analysis, Med. Image Anal. 95 (2024) 103201, http://dx.doi.org/10.1016/j.media.2024.103201.